REVIEW PAPERS

H. Harmuth[1,2], R.C. Bradt[3]

Investigation of Refractory Brittleness by Fracture Mechanical and Fractographic Methods

THE AUTHORS

Harald Harmuth (1957) is professor for ceramics at the University of Leoben, Austria. After his diploma in ceramics in 1980 he spent 16 years with several companies of refractories and cement industry and earned his doctoral degree and his postdoctoral lecture qualification during this time. In the fields of refractories his research interests cover mechanical and chemical material wear including material characterization and simulation.

Richard C. Bradt is the Alton N. Scott Professor of Engineering, Emeritus, at the University of Alabama in Tuscaloosa, Alabama, USA. He is a graduate of MIT and RPI and has taught on the faculties of Penn State University, the University of Washington and now at the University of Alabama. His primary interest is in the fracture mechanics of brittle materials, ceramics, glass and refractories. He is a distinguished life member of UNITECR, the international refractories organization. Prof. Bradt has published nearly 400 papers and advised nearly 50 PhD graduate students.

ABSTRACT

Reduced brittleness is a favorable refractory property for many applications, e.g. in the case of thermal shock. Fracture mechanics and fractographic investigations have been performed in order to clarify some of the mechanisms of brittleness reduction and the essential structure/property relations. Six different basic and nonbasic commercial refractories were considered. The results show that reduced brittleness is mainly achieved by a strength reduction while maintaining the specific fracture energy. This is associated with less transgranular crack propagation and a greater amount of the crack propagation along the grain/matrix boundaries for reduced brittleness.

KEYWORDS

fracture mechanics, refractory brittleness, fractography
Refractories Manual 2010

1 Introduction

For many applications it is desired that refractory materials sustain considerable strain without strength loss to maintain with high residual strength. These strains may originate from the thermal expansion in the case of thermal shock. They may also occur from mechanical loading. An example for the latter is the elliptical deformation of the lining and steel shell of cement rotary kilns. Two different types of refractory material behaviour may help to achieve a high strain bearing capacity. The first is a large strain at crack initiation. In the case of pure linear elastic behaviour this refers to a high ratio of the tensile strength f_t to Young's elastic modulus E. Failure is avoided so long as the imposed strain is lower than f_t/E. By contrast the second type of material behaviour may show crack initiation under severe service conditions, but very limited amount of crack propagation. This maintains a high residual strength. Type one is favourable for the case where crack initiation can definitely be avoided. But if fracture initiation is not avoided then a complete material failure will frequently occur. Therefore type two material behaviour may be considered to be more safely in many refractory applications. Such materials will show a reduced brittleness, and brittleness reduction therefore is a predominant goal of most refractory development.

The definition of "brittleness" unfortunately is not applied unambiguously in the many different fields of materials science. In the case of ordinary ceramic refractory materials it seems most appropriate to define it by the ratio of the elastically stored strain energy at crack initiation to the fracture surface energy necessary for total failure of the material. If this ratio is high then the elastic strain energy may be sufficient for complete material failure without additional energy input. This is what is considered to be "brittle" in every day life: A glass window may fail totally after impact as the ratio quoted above is relatively high. Special measures are necessary to reduce this ratio e.g. in case of impact resistant glass. These explanations already suggest that brittleness will depend on the size of the specimen or the building element, respectively. The elastically stored strain energy is proportional to the volume of the material, but the fracture surface energy to the fracture surface. Therefore the ratio should depend on the first power of a characteristic specimen dimension L.

It can easily be shown that it is proportional to a brittleness number, B, according to the following equation [1]:

$$B = \frac{f_t^2 \cdot L}{G_F \cdot E} \qquad (1)$$

Here G_F is the specific fracture energy which equals the total fracture energy divided by the area of the projection of the fracture surface. For assessment of material brittleness alone without taking specimen size L into consideration a so called charac-

1 Chair of Ceramics, University of Leoben, 8700 Leoben, Austria
2 COMET K2 MPPE Competence Centre, Materials Center Leoben Forschung GmbH, 8700 Leoben, Austria
3 Alton N. Scott Professor, Department Metallurgical and Materials Engineering, 136 Bevill Research Building, The University of Alabama, Tuscaloosa, USA

teristic length l_{ch} is frequently used which is inversely proportional to brittleness number B [1]:

$$l_{ch} = \frac{G_F \cdot E}{f_t^2} \qquad (2)$$

Brittleness reduces with decreasing B and increasing l_{ch}. The characteristic length is proportional to the well known R´´´´ parameter according to Hasselman [2]:

$$R'''' = \frac{\gamma \cdot E}{f_t^2} = \frac{l_{ch}}{2} \qquad (3)$$

where γ is the specific fracture energy relative to the double area of the projection of the fracture surface which causes the denominator of 2 in the above equation. It can be shown that the R´´´´ parameter is significant for the thermal shock behaviour in many loading cases, which confirms the relevance of a decreased brittleness for thermal shock resistance.
Several methods are well known to be effective for brittleness reduction at least for selected material groups. Members of the spinel group help to reduce material brittleness at least for fired basic refractories, magnesia alumina spinel, $MgAl_2O_4$ has been applied for decades. Moreover it is well known that pre-fabricated micro-cracks play an important role for brittleness reduction. In most cases lower brittleness materials have been developed following an empirical route. Investigations documented here aim to elucidate methods influencing material behaviour from a more scientific point of view. Commercially produced refractories of different brittleness have been investigated by fracture mechanics methods and with a microscopic fractographic technique. The combination of both clarifies which mechanisms act to reduce brittleness. They indicate which structure/property relations determine the refractory brittleness and which structural characteristics reduce it. By this a sound scientific basis for further product development is provided.

2 Fracture mechanics test methods

Equation (2) defines the mechanical properties necessary for brittleness assessment. Several static and dynamic procedures are available for Young's elastic modulus determination. For meaningful values at elevated temperatures only the dynamic methods should be applied. In static testing procedures material creep causes underestimation of Young's elastic modulus. For the present investigations a RFDA resonant frequency and damping analyzer device of the company IMCE, Genk/Belgium as well as determination from ultrasonic velocity and bulk density measurement have been applied. They showed satisfactory agreement. For the determination of the specific fracture energy originally notched beam specimens have been used. Stable crack propagation is a necessary precondition for a meaningful result. To facilitate this a chevron notched specimen was designed. Nakayama et al. investigated crack stability for this so called work-of-fracture test [3]. Typical values for the specific fracture energy γ_{WOF} of commercial refractories may e.g. be seen from [4–5]. Although these investigations provided most valuable contributions to refractory fracture mechanics results must not be regarded to be independent from specimen size. Deviations of the material behaviour from pure linear elastic fracture mechanics (LEFM) bring about a size effect which means an increase of the apparent specific fracture energy with rising fracture surface area. Therefore testing facilities which enable stable crack propagation for a large specimen size are desirable. The wedge splitting test according to Tschegg showed to be convenient for this purpose [6–7]. It favours stable crack propagation because of a relatively low ratio of specimen volume to fracture surface area and a reduction of the testing force by the action of a wedge thus decreasing the energy elastically stored in the testing machine [8].

The principle of this test may be seen from Fig. 1. Cubically shaped specimens are equipped with a groove, a starter notch and two side grooves. The groove hosts a load transmission equipment consisting of a wedge, two rolls and two load transmission pieces. It transforms the vertical force of the testing machine F_V into a horizontal force F_H splitting the specimen. During this procedure the loadpoint displacement δ is measured and registered. From the load/displacement diagram the specific fracture energy can be determined by integration:

$$G_F = \frac{1}{A}\int_0^{\delta_{ult}} F_H \, d\delta \qquad (4)$$

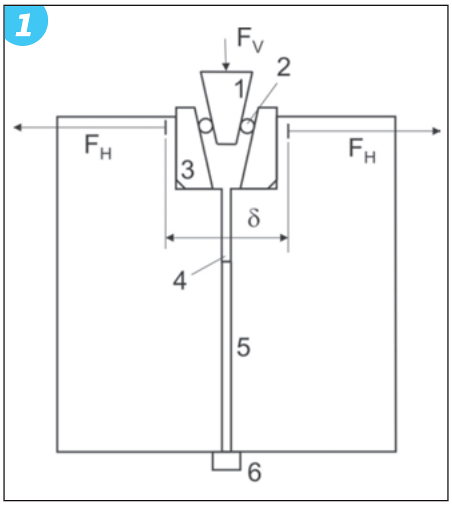

Fig. 1 • Schematic representation of wedge splitting specimen and testing procedure. F_V – vertical load, F_H – horizontal load, δ – displacement, 1 – wedge, 2 – rolls, 3 – load transmission pieces, 4 – starter notch, 5 – side groove, 6 – linear support

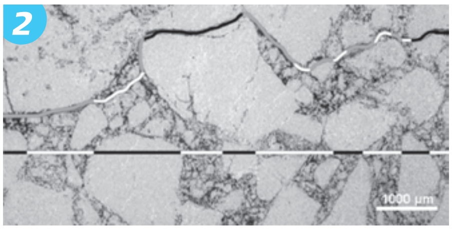

Fig. 2 • Example of a micrograph showing evaluation of the crack path and the lineal analysis; details are explained in the text

where δ_{ult} is the ultimate displacement and A the area of the projection of the fracture surface. From the maximum load $F_{H,max}$ a so called nominal notch tensile strength δ_{NT} can also be determined:

$$\sigma_{NT} = \frac{F_{H,max}}{b \cdot h} \cdot \left(1 + \frac{6y}{h}\right) \qquad (5)$$

In equation (5) b and h are the width and height of the fracture surface area, respectively, and y is the vertical distance of the centre of gravity of the fracture surface from the horizontal force. For the further procedure this nominal notch tensile strength was applied to replace the tensile strength f_t in equation (2).

3 A microscopic fractographic procedure

Wedge splitting tests as shown in section 2 were performed prior to the microscopic fractographic examination for two reasons. On the one hand test results have been necessary for interpretation of fractographic investigations. On the other, specimens after wedge splitting test have been used for fractographic investigation. The following procedure was chosen: After the wedge splitting tests specimen halves still show some adherence and are not totally separated from each other. This occurs because of the tractions in the crack following wake region behind the crack. They are embedded in a synthetic resin and then cut perpendicular to the fracture surface several times. At least three sections per specimen were investigated. These are further ground on abrasive wheels with a fineness down to 20 µm. Sections containing the whole fracture path with a length of approximately 60 mm were photographically documented with a scanning electron microscope. On these digital images the crack path afterwards is coloured to mark three different regions: One is the crack propagation between the grain and the matrix, another crack propagation within the matrix and the third crack propagation within the grain (transgranular crack propagation).
On the same micrographs a lineal analysis was performed. For this purpose several straight lines parallel to the main direction of crack propagation are superimposed to the micrograph. Intercepts of these lines within the grain and within the matrix are coloured differently in order to determine the volume percentage of grain and matrix. Then the coloured pictures are digitally evaluated to determine the lengths of the three different regions. Their percentages relative to the whole crack length or the whole length of the straight lines, respectively, was then calculated. From this procedure the following characteristic figures are determined:

- Crack length along grain/matrix interface $l_{C,GM}$
- Crack length within matrix $l_{C,M}$
- Transgranular crack length $l_{C,G}$
- Volume fracture of grains $l_{L,G}$
- The ratio of the crack length along the grain/matrix interface to the transgranular crack length $l_{C,GM}/l_{C,G}$
- The ratio of the transgranular crack length to the volume fraction of grains $l_{C,G}/l_{L,G}$.

Figure 2 shows an example of a micrograph. To facilitate reproduction the colours are replaced by grey scale values.

4 Refractories investigated and mechanical properties

Five basic and one non basic commercial refractories have been tested. Among the basic materials are two pure fired magnesia bricks, two fired magnesia spinel bricks (one with spinel $MgAl_2O_4$ and one with hercynite $FeAl_2O_4$), and a pitch bonded magnesia carbon brick. The other material is a burned alumina brick with a high alumina content. Some characteristics are shown in Table 1.
All materials were tested at room temperature, additionally material B and C also were investigated at 1100 °C. Refractory E was investigated at room temperature in two ways, in the as-delivered state (E1) and after temperature treatment at 1000 °C under reducing conditions (E2). The most important material properties are shown in Table 2. Only the brittleness related figures are addressed here. At room temperature the pure magnesia materials show the most brittle behaviour as can be seen by the lowest values of l_{ch}. Brittleness reduction by spinel addition is evident and at room temperature more effective for material D compared with material C. Refractories E and F appear to be less brittle than A and B. The firing process for refractory E reduced its brittleness. An even by far lower brittleness exhibits at 1100 °C for materials B and C. The

Table 1 • Some characteristics of materials investigated

A	Pure burnt magnesia brick; 6 mass-% Fe_2O_3		
B1	Pure burnt magnesia brick; 97 mass-% MgO	B2	As B1, at 1100 °C
C1	Burnt magnesia spinel brick; 10.5 mass-% Al_2O_3	C2	As C1, at 1100 °C
D	Burnt magnesia hercynite brick; 3.4 mass-% Al_2O_3		
E1	Pitch bonded magnesia carbon brick; 15 mass-% residual C	E2	As E1, after coking at 1000 °C
F	Burnt alumina brick; 99.3 mass-% Al_2O_3		

Table 2 • Results of mechanical and fracture mechanical investigations

	A	B1	B2	C1	C2	D	E1	E2	F
E / GPa	105	110	80.4	33.8	43.3	33.7	42.8	7.45	88.1
G_F / N/m [1)]	189	168	308	147	435	187	162	257	184
σ_{NT} / MPa	11.8	9.97	3.97	3.91	1.94	3.41	4.54	1.87	7.85
l_{ch} / mm	143	186	1574	325	4982	544	337	546	263
G_F/σ_{NT} / µm	16.0	16.9	77.7	37.7	224	55.0	35.7	137	23.5
σ_{NT}^2/E / kPa	1.32	0.905	0.196	0.453	0.0872	0.345	0.482	0.471	0.700

[1)] Figures for specific fracture energy and quantities calculated form it (also in Table 4) have been erroneously reported in [9–10] and are corrected hereby characteristic length is increased by more then a factor of 10. It can be observed that the ratio G_F/σ_{NT} shows the same and the ratio σ_{NT}^2/E the inverse trend as the characteristic length l_{ch}. The latter ratio is proportional to the elastic strain energy stored in the specimen at crack initiation.

5 Results of microscopic fractographic investigations

The main results of the microscopic fractographic investigations may be seen from Table 3. The most brittle materials A and B1 exhibit the highest amount of transgranular crack propagation. With decreasing brittleness the amount is reduced in favour of crack propagation along the grain/matrix interface. The amount of crack propagation within the matrix shows no significant trend. The relation between brittleness and transgranular crack propagation for the materials investigated here is the main result. It is also clearly visible from the ratio $l_{C,GM}/l_{C,G}$ which shows its lowest values for the most brittle materials A and B1. For the materials investigated here this relation does not significantly depend on the volume fraction of the grains, and the ratio $l_{C,G}/l_{L,G}$ shows a positive trend with brittleness and is mainly determined by the numerator.

6 Discussion of results

Table 4 is a correlation matrix for some of the most important results. Only the room temperature measurements of as delivered materials have been evaluated. Of course just a few parameters show a significant correlation (i.e. a value close to –1 or 1). This is e.g. the case for the nominal notch tensile strength and the Young's elastic modulus. Contrary to this, the nominal notch tensile strength and the specific fracture energy show no significant correlation, which is of special importance and will be addressed later.

It can be observed from Table 4 l_{ch} and G_F/σ_{NT} are equivalent brittleness measures. Moreover G_F/σ_{NT} shows a negative correlation with σ_{NT} and no significant correlation with G_F. From this it can be concluded that a decrease of brittleness (increase of ratio G_F/σ_{NT}) is achieved by a reduction of strength (decrease of σ_{NT}). Stronger is not always better. Further the amount of transgranular crack propagation $l_{C,G}$ shows a positive correlation with σ_{NT}. These correlations show that brittleness reduction, i.e. increase of characteristic length l_{ch}, is for the materials investigated here typically achieved by a strength decrease while maintaining the specific fracture energy. This issue raises two important questions. One concerns the methods and mechanisms of strength decrease. The other regards how it is possible to maintain specific fracture energy, i.e. to avoid its decrease, when the strength is reduced. The first question will be further addressed now. As shown by the results and correlations above, lower strength is related to a higher amount of crack propagation along the grain/matrix boundary and a lower amount of transgranular crack propagation. This is reasonable as the grains usually are the structural element with the highest strength. Several reasons may cause the crack to propagate predominantly not in a transgranular manner. In the case of refractory E, the interface strength of the carbon/magnesia bond is supposed to be considerably lower than the strength of the magnesia itself, and therefore failure along the grain/matrix bond is favoured. After coking at 1000 °C pore rims around the magnesia grains develop, thus largely reducing Young's elastic modulus as can be seen from Table 2, and even more enhancing crack propagation along the grain/matrix interface. In case of spinel containing burnt refractories micro-cracks are prefabricated during the cooling period of the firing process. They are caused by a mismatch between the thermal expansion of magnesia and spinel, the latter being far lower. Micro-cracks are primarily formed along the grain/matrix boundary and within the matrix and therefore reduce the amount of transgranular crack propagation.

The second question quoted above is brought about by LEFM. According to Irwin's similarity relation the critical stress intensity factor and therefore the strength would be proportional to the square root of the specific fracture energy. Therefore a strength decrease should be associated with a decrease of specific fracture energy. This is not the case for the materials investigated here according to Table 4. Moreover, it can be shown that under assumption of pure linear elastic material behaviour the characteristic length l_{ch} would approximately be equal to the flaw size multiplied with a constant of the order of magnitude of $\pi/2$. More details may be seen from [11]. For ordinary ceramic refractory materials this would result in a characteristic length in the order of magnitude of less than 10mm. As can be seen from Table 2 this is at least one power of ten lower than actually measured values. Therefore, deviations from pure LEFM are essential. These are from energy consuming processes before (frontal process zone) and behind (following wake) the crack tip. A schematic representation is shown in Fig. 3. Especially grain bridging and friction of crack faces are able to consume energy in the wake, micro-cracking may also occur the frontal process zone. Moreover irreversible inelastic deformation is expected to contribute at elevated temperatures. Different methods may help to estimate length

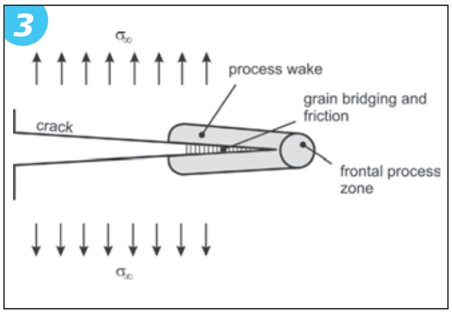

Fig. 3 • Schematic representation of micro-processes in the vicinity of the crack tip; σ_∞ – external loading

Table 3 • Results of microscopic fractographic investigations

	A	B1	B2	C1	C2	D	E1	E2	F
Crack									
a) at grain/matrix interface / %	32.2	38.6	59.8	49.7	57.8	44.9	63.7	73.5	55.1
b) within matrix / %	38.0	38.4	29.8	42.1	32.2	43.9	31.6	23.1	32.7
c) within grain / %	29.8	23.0	10.5	8.2	10.0	11.2	4.7	3.42	12.2
Volume fraction of grains / vol.-%	58.9	62.8	64.9	50.6	53.6	51.5	53.0	55.8	62.7
Crack length grain/matrix: transgran. crack length	1.08	1.68	5.71	6.07	5.79	4.01	13.4	21.5	4.53
Transgran. crack length: volume fraction of grains	0.507	0.366	0.161	0.162	0.186	0.217	0.0893	0.0612	0.194

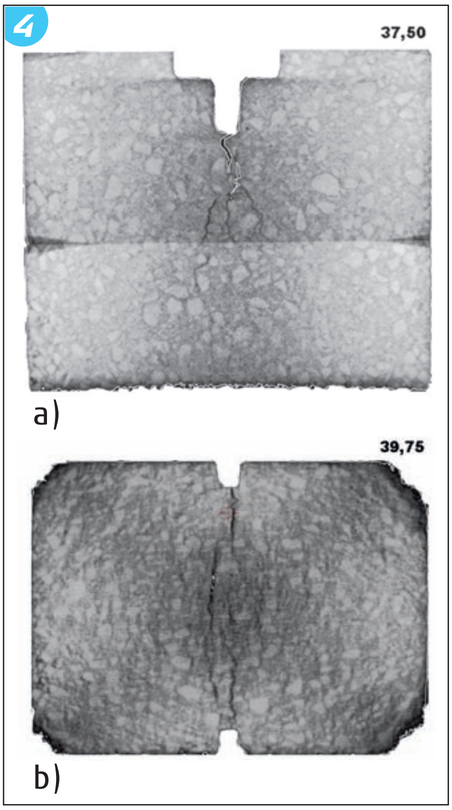

Fig. 4 • Computer tomographic image of a vertical a) and a horizontal b) section of material C1 after wedge splitting test

Table 4 • Correlation matrix for some of the results

	E	G_F	σ_{NT}	l_{ch}	G_F/σ_{NT}	σ_{NT}^2/E	$l_{C,G}$	$l_{C,G}/l_{L,G}$
E	1							
G_F	0.42	1						
σ_{NT}	0.97	0.42	1					
l_{ch}	-0.84	0.02	-0.88	1				
G_F/σ_{NT}	-0.91	-0.10	-0.91	0.98	1			
σ_{NT}^2/E	0.88	0.40	0.97	-0.86	-0.86	1		
$l_{C,G}$	0.84	0.49	0.91	-0.68	-0.70	0.93	1	
$l_{C,G}/l_{L,G}$	0.77	0.49	0.87	-0.62	-0.63	0.90	0.99	1

and width of process zones. Length of process wake and frontal process zone may be estimated from the ascending and descending part of R-curves. Details about R-curve measurement can be found in [12]. Estimation of process zone width by acoustic emission measurements for the wedge splitting test is shown in [13]. Here only a visual inspection by computer tomography is addressed. Figure 4 shows a vertical and a horizontal section through a wedge splitting specimen of material C1 after the test. Both show multiple crack branching, and especially, the horizontal section exhibits some micro-cracking.

How can the above considerations contribute to clarify why specific fracture energy is maintained while strength is reduced at the same time? Strength and brittleness reduction are related to a larger portion of the crack path propagating along the grain/matrix interface. This causes a more "tortuous" crack path. Crack tortuosity and its contribution to specific fracture energy was already addressed earlier [4]. It brings about friction of crack faces, grain bridging and interlocking in the following wake region. Moreover in the case of reduced brittleness a flaw structure present at the grain/matrix boundary gives rise to micro-cracking, further propagation of micro-cracks and crack branching. These processes and the associated process zone contribute to the specific fracture energy and support to maintain its value when strength is reduced.

7 Outlook

Investigations presented here help to clarify the microstructural processes enabling the decrease of refractory brittleness. From these findings of material development, it is suggested one should concentrate on the design of the grain/matrix interface strength in order to tailor material brittleness. Moreover the effectiveness of measures taken may be assessed by both fracture mechanics and fractographic methods.

Acknowledgement

Financial support by the Austrian Federal Government (in particular from the Bundesministerium für Verkehr, Innovation und Technologie and the Bundesministerium für Wirtschaft und Arbeit) and the Styrian Provincial Government, represented by Österreichische Forschungsförderungsgesellschaft mbH and by Steirische Wirtschaftsförderungsgesellschaft mbH, within the research activities of the K2 Competence Centre on "Integrated Research in Materials, Processing and Product Engineering", operated by the Materials Center Leoben Forschung GmbH in the framework of the Austrian COMET Competence Centre Programme, is gratefully acknowledged. Further the authors thank I. Petschenig for contributing to the laboratory investigations.

References

[1] **Harmuth, H., Tschegg, E.K:** A fracture mechanics approach to the development of refractory materials with reduced brittleness. Fatigue Fract. Engine Mater. Struct. **20** (1979) 1585–1603

[2] **Hasselman, D.P.H.:** Unified theory of thermal shock fracture initiation and crack propagation in brittle ceramics. J. Amer. Ceram. Soc. **52** (1969) 600–604

[3] **Nakayama, J., Abe, H., Bradt, R.C.:** Crack stability in the work-of-fracture test; refractory applications. J. Amer. Ceram. Soc. **64** (1981) 671–675

[4] **Uchno, J.J., Bradt, R.C., Hasselman, D.P.H.:** Fracture surface energies of magnesite refractories. Ceram. Bull. **55** (1976) 665–668

[5] **Ainsworth, J.H., Herron, R.H.:** High temperature fracture energy of refractories. Ceram. Bull. **55** (1976) [7] 655–664

[6] Tschegg, E.K.: Testing device and appropriate specimen shapes for tests to measure fracture values (in German), Austrian Patent Specification AT 390 328

[7] **Tschegg, E.K.:** New equipments for fracture tests on concrete. Materialprüfung. **33** (1991) 338–342

[8] **Harmuth, H.:** Stability of crack propagation associated with fracture energy determined by wedge splitting specimen. Theoretical and Applied Fracture Mechanics **23** (1995) 103–108

[9] **Harmuth, H.:** Flexibility of refractories – fracture mechanical and microscopic investigations. Proceedings of the 4th International Scientific Conference Refractories, Furnaces and Thermal Insulations, 20.–22. April 2010, Novy Smokovec, Slovakia, (2010) 36–41

[10] **Harmuth, H.:** Characterisation of the fracture path in 'flexible' refractories. 12th International Ceramics Congress CIMTEC 2010, June 6–11, Montecatini Terme, Italy

[11] **Harmuth, H.:** Refractories with reduced brittleness – fracture mechanical considerations. In: G.C. Sih (ed.), Role of Mechanics for Development of Science and Technology, Tsinghua University Press, Beijing, China, (2000) 873–888

[12] **Sakai, M., Bradt, R.C.:** Graphical methods for determining the nonlinear fracture parameters of silica and graphite refractory composites. In: R.C. Bradt and A.G. Evans (eds.), Fracture Mechanics of Ceramics, Plenum, New York, (1986) [7] 127–142

[13] **Tschegg, E.K., Fendt, K.T., Manhart, Ch., Harmuth, H.:** Uniaxial and biaxial fracture behaviour of refractory materials. Engineering Fracture Mechanics **76** (2009) 2249–2259

Received: 20.08.2010